

All-in-One Shape-Adaptive Self-Charging Power Package for Wearable Electronics

Hengyu Guo,^{†,‡,⊥} Min-Hsin Yeh,^{†,§,⊥} Ying-Chih Lai,^{†,⊥} Yunlong Zi,[†] Changsheng Wu,[†] Zhen Wen,[†] Chenguo Hu,^{*,‡} and Zhong Lin Wang^{*,†,||}

[†]School of Materials Science and Engineering, Georgia Institute of Technology, Atlanta, Georgia 30332-0245, United States

[‡]Department of Applied Physics, Chongqing University, Chongqing 400044, China

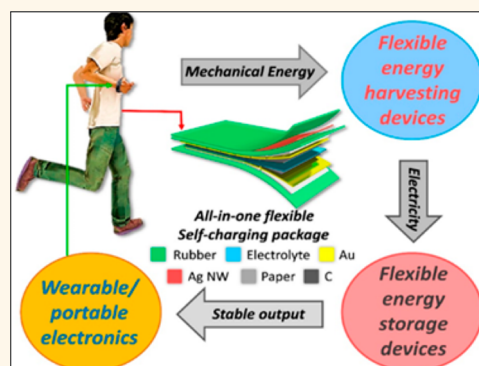
[§]Department of Chemical Engineering, National Taiwan University of Science and Technology, Taipei 10607, Taiwan

^{||}Beijing Institute of Nanoenergy and Nanosystems, Chinese Academy of Sciences, National Center for Nanoscience and Technology (NCNST), Beijing 100083, P. R. China

S Supporting Information

ABSTRACT: Recently, a self-charging power unit consisting of an energy harvesting device and an energy storage device set the foundation for building a self-powered wearable system. However, the flexibility of the power unit working under extremely complex deformations (e.g., stretching, twisting, and bending) becomes a key issue. Here, we present a prototype of an all-in-one shape-adaptive self-charging power unit that can be used for scavenging random body motion energy under complex mechanical deformations and then directly storing it in a supercapacitor unit to build up a self-powered system for wearable electronics. A kirigami paper based supercapacitor (KP-SC) was designed to work as the flexible energy storage device (stretchability up to 215%). An ultrastretchable and shape-adaptive silicone rubber triboelectric nanogenerator (SR-TENG) was utilized as the flexible energy harvesting device. By combining them with a rectifier, a stretchable, twistable, and bendable, self-charging power package was achieved for sustainably driving wearable electronics. This work provides a potential platform for the flexible self-powered systems.

KEYWORDS: triboelectric nanogenerators, supercapacitors, wearable electronics, self-charging power package, kirigami



Flexible wearable/portable electronics, such as bendable displays,^{1–3} stretchable circuits,^{4–7} e-skins,^{8–10} and e-papers,¹¹ are receiving intensive attention due to their huge applications in medical science, robotics, and human–machine interface. For powering these electronics, a lightweight supply module with complex deformation properties (e.g., bending, stretching, and torsion) is desirable.^{12–14} Various platforms, such as paper-based,^{15–19} fiber-like, buckling-type, and origami-architecture^{20–23} flexible supercapacitor/battery systems, have been proposed to achieve this. For current commercialized power platforms, supercapacitors offer extraordinary advantages over conventional charging battery systems, including high charging rate, long life cycles, and high reliability.²⁴

One of the bottlenecks for utilizing flexible supercapacitors to power up wearable/portable electronics is insufficient operating time. To address this issue, our group has creatively proposed and demonstrated several energy harvesting systems based on the mechanisms of piezoelectric,^{25–27} pyroelectric,²⁸ and triboelectric charging.^{21,29–32} Based on the coupling between triboelectrification and static-electric induction, a triboelectric

nanogenerator (TENG) has shown advantages of high output, high energy conversion efficiency, lightweight, flexibility,^{21,33} and shape-adaptive stretchability,^{34,35} which serves as an ideal strategy to scavenge mechanical energy from low-frequency³⁶ irregular body motions.^{24,37–40} By integration of TENGs with a battery/supercapacitor unit, self-charging power units (SCPU) have been demonstrated to sustainably power electronics.^{24,33,41,42} However, to be utilized in extremely harsh operating circumstances, for example, stretching, twisting, and folding, a fully shape-adaptive flexible and stretchable SCPU is still required to be developed.

Here, we present a prototype of an all-in-one shape-adaptive SCPU that can be used for harvesting body motion energy under complex mechanical deformations (e.g., stretching, twisting, and bending) and building a self-powered system for wearable electronics. By taking advantages of kirigami

Received: September 30, 2016

Accepted: November 7, 2016

Published: November 7, 2016

architecture,^{43–45} a paper based graphite electrode can be designed with different geometric numbers (4–12 units). Kirigami paper based supercapacitors (KP-SCs) show proportional stretchability up to 215% with excellent mechanical durability (2000 stretching/releasing cycles) and reliability (5000 charging/discharging cycles). By utilizing silicone rubber and Ag nanowires (AgNWs), an ultrastretchable and shape-adaptive silicone rubber TENG was proposed and fabricated with an output of ~ 160 nC per half working cycle and open-circuit voltage of ~ 250 V under stretching state of 100%. By assembling the KP-SC into the TENG with a full-wave rectifier, an all-in-one shape-adaptive SCPU was achieved, which is stretchable, bendable, and twistable. At last, we successfully demonstrate this power unit for harvesting hand flapping energy and continually powering an electric watch to realize the whole self-powered system. Moreover, with the components sealed in silicon rubber, our proposed SCPU is also washable and can be integrated into fabrics.

RESULTS AND DISCUSSION

Design of the All-in-One Shape-Adaptive Self-Charging Power System for Wearable Electronics. The system of all-in-one shape-adaptive self-charging power unit for driving the wearable/portable electronics is schematically illustrated in Figure 1. Our proposed all-in-one shape-adaptive self-charging

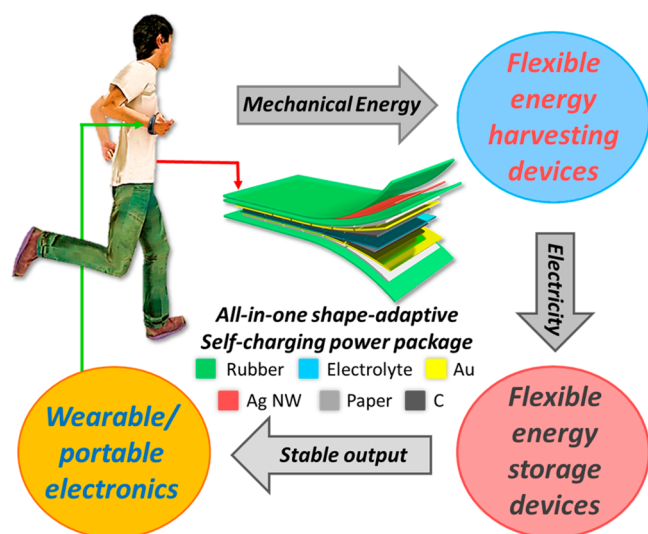


Figure 1. Working mechanism of an all-in-one shape-adaptive self-charging package for wearable/portable electronics. Mechanical energy from human motions can be harvested and then converted to electricity by an all-flexible silicone rubber based triboelectric nanogenerator and then stored into a kirigami based supercapacitor for driving wearable and portable electronics. The layer-by-layer schematic illustration of all-in-one shape-adaptive self-charging package is shown in the center.

power unit can be easily fixed on the cloth or even placed in conventional textiles for scavenging the mechanical energy originating from body movement via an all-flexible silicone rubber based TENG. Meanwhile, the generated AC electric energy can be directly stored in a kirigami paper based supercapacitor (KP-SC) after rectifying with an all-wave rectifier for sustainably driving wearable/portable electronics. The layer-by-layer schematic structure of an all-in-one shape-adaptive self-charging power unit has been shown in the center of Figure 1. Before the concurrent operations of our-proposed

all-in-one shape-adaptive self-charging power unit, the characterization of each functional device was carried out individually to evaluate its performance one by one.

Preparation and Characterization of the Flexible Kirigami Paper Based Supercapacitor. The flexible energy storage unit is the key to solving the limitations of current flexible energy storage devices under extremely harsh operating circumstances, for example, stretching, twisting, and folding. Here, an ultralight and superflexible paper based supercapacitor was designed and fabricated utilizing the concept of kirigami architecture, as depicted in Figure 2. First, sandpaper was used as the substrate due to its extremely rough surface (as shown in Figure S1a) for increasing the loading amount of active material and waterproof property for electrolyte assembling. The kirigami based sandpaper electrode can be precisely designed and then fabricated by laser cutter. After that, a conductive Au layer (thickness ~ 200 nm) was deposited on the surface of the kirigami based sandpaper electrode by e-beam deposition. In this study, graphite was utilized as the active material in the KP-SC device and then directly coated on as-prepared laser-patterned electrode by the common pencil drawing method.⁴⁶ The detailed fabrication process for KP-SC is shown in Figure 2a and explained in the Experimental Section. Figure 2b shows the layer-by-layer schematic illustration of the KP-SC unit. For realizing the stretchable characteristic, the cellulose paper based spacer between the two identical kirigami graphite electrodes was also patterned with the same feature by laser cutter. The surface morphology of the KP-SC electrode is shown in inset 1 of Figure 2b, which revealed that the porous and rough structure of graphite creates a high active surface area and better electrolyte penetration.⁴⁶ Meanwhile, the cross-section SEM image of the KP-SC electrode is also exhibited as inset 2, which clearly demonstrated a layer-structured KP-SC electrode containing ~ 15 μm graphite layer and a ~ 200 nm Au deposited layer on sandpaper substrate (~ 45 μm). It is also worth mentioning that our proposed superthin (<250 μm) and ultralight (<55 mg/cm^2) KP-SC provides a promising strategy for replacing the conventional bulky energy storage unit in the application of the wearable/portable electronics. Figure 2c shows the schematic illustration and related maximum tensile strains of KP-SCs with different kirigami geometric unit numbers from 4 to 12 units (the definition of maximum tensile strain for KP-SC is described in Figure S1b),⁴⁴ which shows that the maximum tensile strain for KP-SC will proportionally increase with increasing the geometric unit number from 4 to 12 units. It is noteworthy that the maximized stretchability of KP-SC can be up to 215% when the kirigami geometric unit number reaches 12. However, the conductivity of the KP-SC electrode will also be sacrificed after enlarging its maximum stretchability, as shown in Figure 2d. For the optimization between the stretchability and conductivity of the KP-SC, KP-SC device with kirigami geometric unit number of 6 will be utilized in following study and discussion. The relationship between the resistance and the strain of the KP-SC with kirigami geometric unit number of 6 is shown in Figure S1c. To demonstrate the characteristics of the flexible KP-SC under extremely harsh operating circumstances, three photographs of the KP-SC under stretching, twisting, and bending deformation were taken as shown in Figure 2e,f,g, respectively. Above results provide a promising picture to utilize our proposed stretchable KP-SC in flexible wearable/portable electronics.

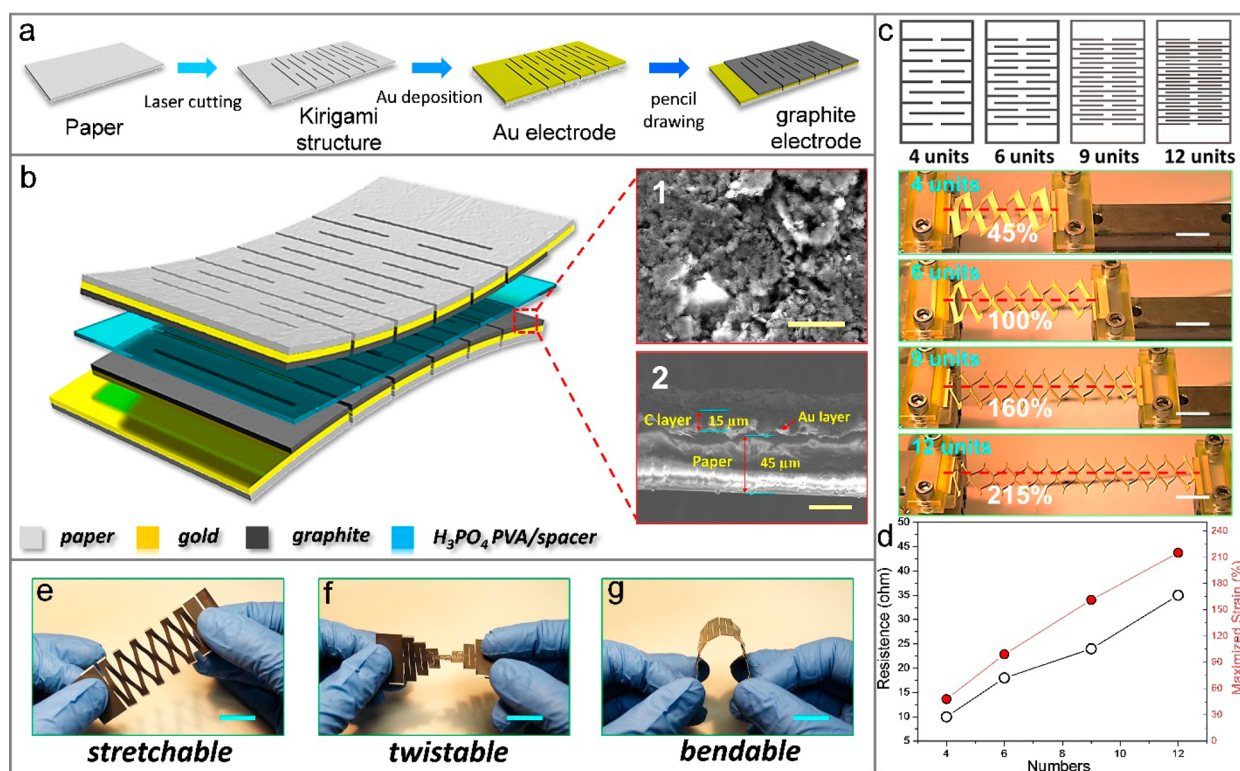


Figure 2. Schematic illustration and mechanical behaviors of a kirigami based supercapacitor. (a) Preparation process of kirigami based electrode. (b) Schematic structure of a kirigami based supercapacitor (KP-SC). The SEM image of the (1) cross-section (scale bar $30\ \mu\text{m}$) and (2) top (scale bar $10\ \mu\text{m}$) of the kirigami based electrode are shown as insets. (c) Schematic illustration of kirigami based electrodes with different geometric unit numbers (4–12); the related strain property of these kirigami based electrodes is also examined as shown in photographs. (scale bar 1 cm). (d) Dependence of resistance and maximal strain of the kirigami based electrode with different geometric unit numbers. (e–g) Photographs of the KP-SC under various mechanical deformations, stretching, twisting, and bending (scale bar 1 cm).

Performance of the Flexible Kirigami Paper Based Supercapacitor for Energy Storage.

The electrochemical capacitance properties of a KP-SC device were evaluated by cyclic voltammetry (CV) and galvanostatic charging/discharging (GCD) techniques. All of the electrochemical performances of the KP-SC device were measured by a symmetric configuration of two identical graphite loaded kirigami electrodes with a solid state H_3PO_4 /poly(vinyl alcohol) (PVA) as the electrolyte. To evaluate the fast charge/discharge ability of the KP-SC, CV at different scan rates from 10 to 100 mV/s were examined, as shown in Figure 3a. It can be observed that the rectangular CV curves do not distort significantly as the scan rate increases, indicating its good capacitive behavior and high-rate charging capability. Figure 3b also shows the GCD curves of the KP-SC under various current densities from 20 to $50\ \mu\text{A}/\text{cm}^2$ in the potential range from 0 to 0.8 V. The specific surface capacitance calculated from the GCD curves at different CD rate is also shown in Figure S2b. Figure 3b reveals that no obvious IR-drop behavior was observed even at a fast discharging rate ($50\ \mu\text{A}/\text{cm}^2$), indicating the outstanding capacitance behavior and excellent conductivity of the graphite based electrode. Moreover, the Nyquist plot of the KP-SC was also examined by electrochemical impedance spectroscopy (EIS), as presented in Figure S2a. The magnitude of equivalent series resistance (ESR) of $20.99\ \Omega$ is obtained from the x -intercept of the Nyquist plot. The specific mass (F/g) and surface capacitance (mF/cm^2) calculated from the CV curve at the corresponding scan rate are shown in Figure 3c. The specific capacitance was found to decrease with increasing scan

rate since the incomplete charging/discharging of the electrode material was limited by ionic diffusion.³³ The mass and surface capacitance of KP-SC is about $\sim 12\ \text{F}/\text{g}$ and $\sim 1\ \text{mF}/\text{cm}^2$ at the scan rate of 10 mV/s, respectively; these results are similar to the previous work on graphite paper based supercapacitors.⁴⁶ Long-term stability of the supercapacitor is also a critical issue for utilizing in self-powered systems. The inset of Figure 3c shows the cycling performance of the KP-SC during 5000 cycles at a CD rate of $100\ \mu\text{A}/\text{cm}^2$. No obvious capacitance drop was observed after 5000 cycles under such higher CD rate, which provides a reliable stability to introduce in the high-frequency charge/discharge powering systems.

As a stretchable energy storage device, the electric storage performance of KP-SC under different mechanical tensile strains (0–100%) also needs to be investigated and discussed. Figure 3d shows the CV curves of KP-SC under continuous mechanical tensile strains changed from 0 to 100% at a scanning rate of 50 mV/s. Similar CV curves provide solid evidence to prove that the performance of KP-SC was quite stable under any shape deformation. The same result can be also obtained by the corresponding CD curves of KP-SC under CD rate of $30\ \mu\text{A}/\text{cm}^2$, as shown in Figure S2c. A video that demonstrated the CV and CD performance of KP-SC under continuous stretching/releasing movement is shown in Video S1. Furthermore, the Nyquist plot of KP-SC under various tensile strains was also examined and is presented in Figure S2d. The result reveals that the value of EPR for KP-SC was barely changed under different tensile strains (Figure S2e), which implied that the conductivity of KP-SC electrode is not

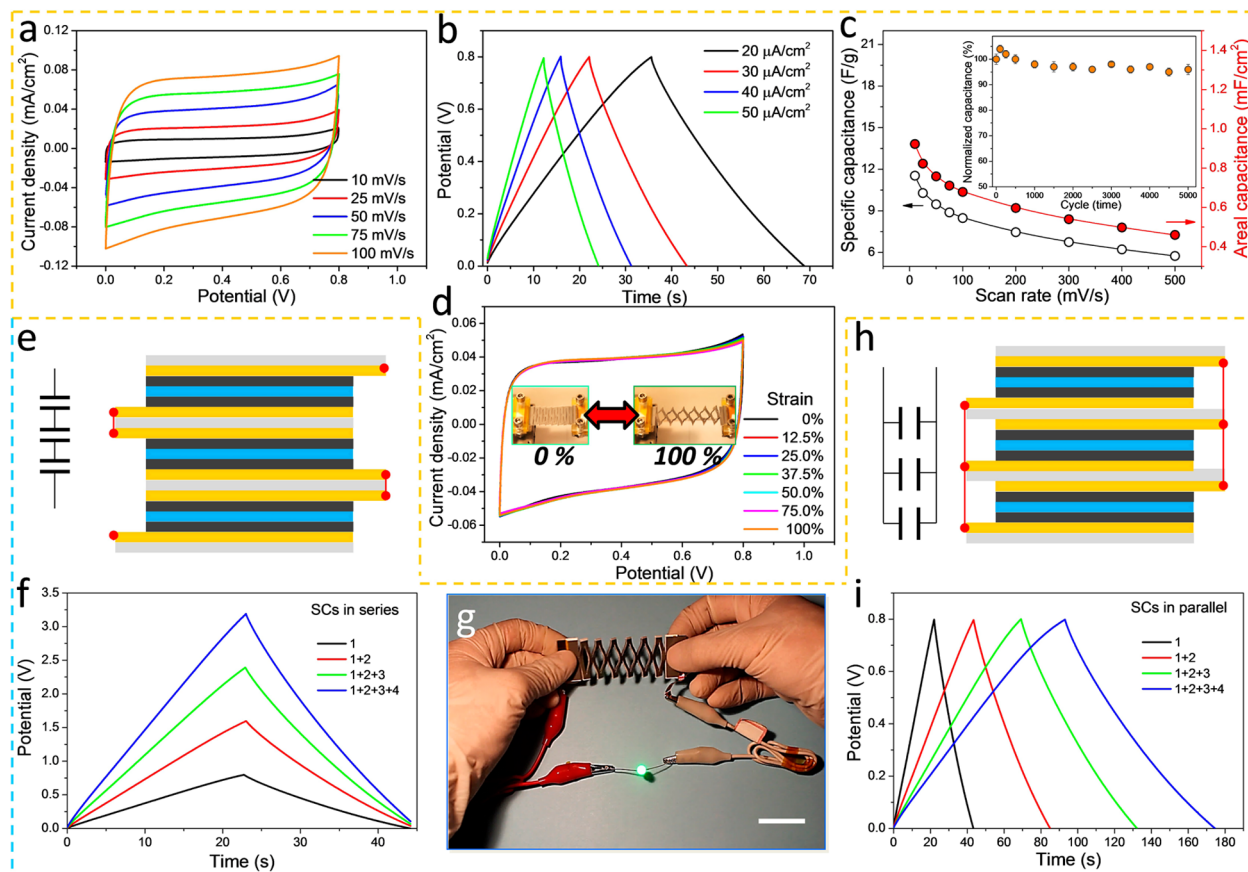


Figure 3. Performance of the kirigami based supercapacitor for energy storage. (a) CV curves of the KP-SC (6 units) under various scanning rates (10–100 mV/s). (b) Galvanostatic charge/discharge (C/D) curves of the KP-SC (6 units) at different current density (20–50 $\mu\text{A}/\text{cm}^2$). (c) Specific mass and surface capacitance of the KP-SC (6 units) under various scanning rates; long-term stability test of the KP-SC (6 units) for 5000 charging/discharging cycles is also shown as the inset. (d) CV curves of the KP-SC (6 units) under mechanical strain changing from 0–100%. The inset shows the photographs of the KP-SC (6 units) under rest (strain = 0%) and stretched states (strain = 100%). (e) Schematic illustration of integrated KP-SCs in series. (f) C/D curves of the integrated KP-SC (6 units) under various number of devices in series connection (1–4 devices) at current density of 30 $\mu\text{A}/\text{cm}^2$. (g) Photograph of using the integrated KP-SC (6 units, 3 devices in series) to light up a single commercial green LED under cycling stretching movement. (h) Schematic illustration of integrated KP-SCs in parallel. (i) C/D curves of the integrated KP-SC (6 units) under various number of devices in parallel connection (1–4 devices) at current density of 30 $\mu\text{A}/\text{cm}^2$. $\text{H}_3\text{PO}_4/\text{PVA}$ based solid state electrolyte was used in KP-SC for all of electrochemical measurements.

influenced by strain deformation. At last, the mechanical durability of KP-SC under 2000 continuous stretching/releasing cycles was also measured and is presented in Figure S2f. According to above results, now it is fair to say that our proposed KP-SC has an excellent stretchability and mechanical durability for utilizing in flexible wearable/portable electronics. Having presented this excellent stretchable supercapacitor, we have further integrated several KP-SC units into assemblies both in series and in parallel connection to meet specific energy needs for practical applications. Figure 3e shows the schematic illustration of four individual KP-SC units connected in series. The GCD and CV curves of series-connected KP-SC with different connected units (1–4) are shown in Figure 3f and Figure S3a, respectively. The output voltage of the series-connected KP-SC linearly increases with increasing the unit number of connected KP-SC units, which provides a tunable operating voltage for driving various types of flexible electronics. Figure 3g and Video S2 demonstrate the highly flexible characteristic of the series-connected KP-SC for lighting up a commercial green LED under extremely harsh operating circumstances, stretching, twisting, and bending. Also, KP-SC units can be connected into an integrated KP-SC module in

parallel configuration for enlarging its capacitance. The GCD and CV curves of parallel connected KP-SC with different connected units (1–4) are shown in Figure 3i and Figure S3b, respectively. All of these results show the tunable adaptability and reliable scalability of the KP-SC to practical applications.

Preparation and Characterization of the Shape-Adaptive Silicone Rubber Based Triboelectric Nanogenerator for Energy Harvesting. For preparing the shape-adaptive triboelectric nanogenerator for harvesting human mechanical energy, ultrastretchable silicon rubber (Smooth-On, Ecoflex 00-10) was selected as the triboelectric material. Silver nanowire (Ag NWs, diameter ≈ 115 nm and length = 20–50 μm) networks were used as the conducting matrix owing to their superior merits of excellent conductivity and ultrahigh stretchability for fabricating the stretchable electrode.^{5–7} Figure 4a shows the structural scheme of the all-flexible silicone rubber based TENG. An SEM image of the Ag NW networks formed on the silicon rubber substrate is also presented as the inset. The detailed fabrication process is shown in Figure S4 and described in the Experimental Section. Ag NW networks create a conductively stretchable electrode, which will not be blocked under extremely strain deformation.

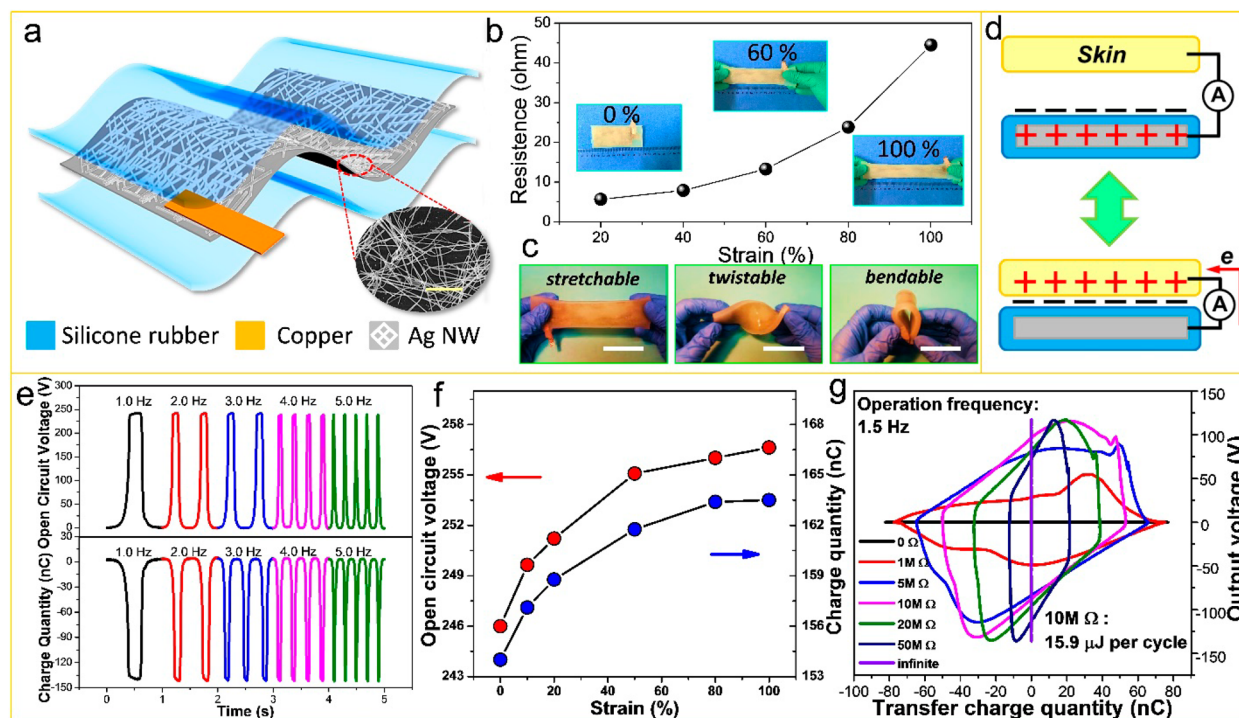


Figure 4. Performance of silicone rubber based triboelectric nanogenerator for harvesting mechanical energies. (a) Structural scheme of the silicone rubber based flexible triboelectric nanogenerator (TENG). The SEM image of the as-prepared Ag nanowires (Ag NWs; $D \approx 115$ nm, $L = 20\text{--}50$ μm) for fabricating the stretchable electrode is shown as the inset (scale bar 20 μm). (b) Dependence of resistance of the Ag NW based electrode under various strain (0–100%). (c) Photographs of the TENG under various mechanical deformations, stretching, twisting, and bending (scale bar 5 cm). (d) Working mechanism of a TENG for harvesting mechanical energy via basic contact-separation mode (here, skin acts as the other electrode in this system). (e) Open circuit voltage (V_{OC}) and short circuit charge transfer (Q_{SC}) of TENG under different working frequencies (1.0–5.0 Hz). (f) Dependence of the value of V_{OC} and Q_{SC} for TENG under different mechanical strains (0–100%). (g) V – Q curves of TENG under connections with various external load (0–50 M Ω).

Hence, such an electrode provides a reliable conductive substrate (~ 50 Ω) for use in the TENG system under different tensile strain states, as shown in Figure 4b. The strain–stress property of the silicone rubber based stretchable electrode and the kirigami based electrode was measured as shown in Figure S5. Figure 4c demonstrates the TENG under different kinds of complex deformations, including stretching, twisting, and bending. The working mechanism of contact-mode TENG is demonstrated in Figure 4d, which utilizes the conjunction of triboelectrification and electrostatic induction.²¹ Briefly, due to their diverse triboelectric polarities, silicone rubber will acquire a negative charge while the skin makes full contact with it. Meanwhile, the surface of the skin will also produce the same amount of positive charges. Once the skin starts to separate from the silicone rubber, the positive charges on the skin will transfer to the AgNW based electrode through the external circuit thus producing current output to balance the potential difference established between the two electrodes. Mechanical motion can easily induce the random contact/separation movement between the skin and silicone rubber, while the TENG has been placed on the cloth. It is noteworthy that the skin is treated as the other electrode of our proposed TENG system, instead of connecting the other electrode to the ground in the common case. According to the previous works,⁴⁷ this kind of connective strategy can further enhance the transferred charge output of TENG and then facilitate the charging process of supercapacitor. Figure 4e shows the basic output performance of open-circuit voltage (V_{OC}) and short circuit charge transfer (Q_{SC}) for the TENG under different operating frequencies

(from 1 to 5 Hz). From the results, the V_{OC} of ~ 250 V and Q_{SC} of ~ 150 nC for TENG were achieved and were barely affected by the working frequency. Moreover, both values can be changed to some extent under various straining states, as shown in Figure 4f, which could be attributed to the Poisson ratio and the electrostatic induction.⁴⁸ While applying the strain force on the two ends of the silicone rubber, the thickness of the TENG along the z -axis will decrease because the volume of the object is the same under both releasing and stretching states (schematic illustration is presented in Figure S6). As a consequence, the charges on the covered electrode will be easily induced by the thinner silicone rubber, thus to some extent enhancing the corresponding value of the Q_{SC} . Furthermore, in this work, the V – Q curve⁴⁹ was employed to evaluate the maximized output energy of TENG per cycle under the working frequency of 1.5 Hz, as shown in Figure 4g. Under the external load of 10 M Ω , a maximized energy of 15.9 μJ (average power of 10.6 μW) for TENG per cycle was achieved, which is high enough to light up several LEDs connected in series (Figure S7).

Demonstration of the All-in-One Shape-Adaptive Self-Charging Power Package for Wearable Electronics. By connecting the TENG to the KP-SC with an all-wave rectifier, an all-in-one shape-adaptive self-charging power unit was achieved after assembling all of the units by a silicone rubber sealing process. Various kinds of human motion can be harvested and then stored into the energy storage part as a sustainable energy supply for driving wearable/portable electronics. The proposed scheme of all-in-one shape-adaptive

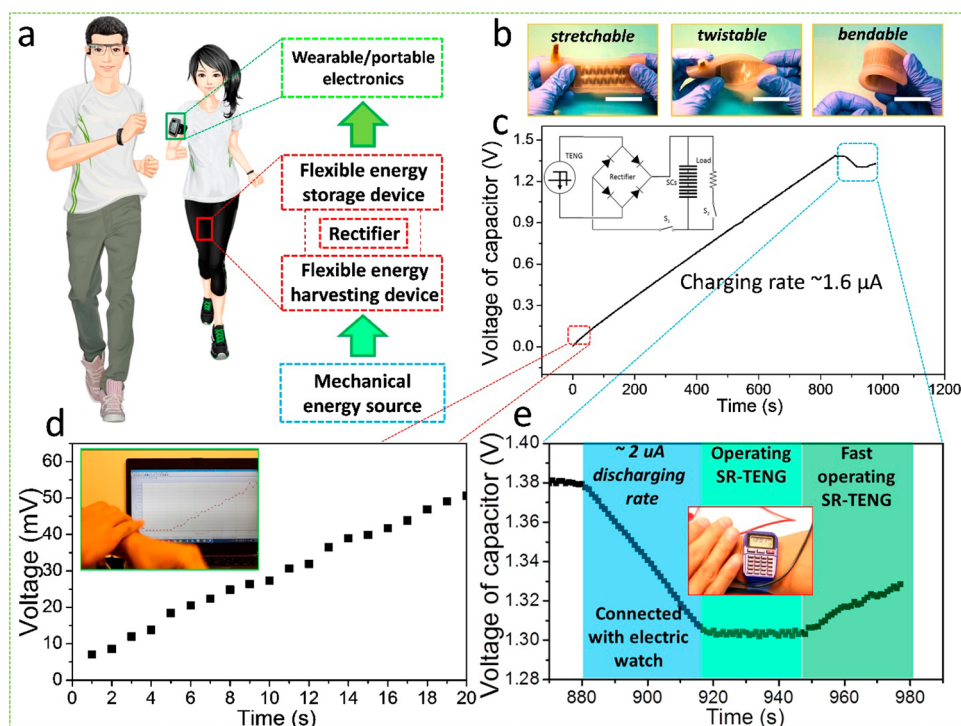


Figure 5. Application of the all-in-one shape-adaptive self-charging power package in conventional wearable electronics. (a) Systematic configuration of the all-in-one shape-adaptive self-charging power clothes for scavenging the mechanical motion energy from the body and then powering the wearable electronics directly. (b) Photographs of the all-in-one shape-adaptive self-charging power package under various mechanical deformations, stretching, twisting, and bending (scale bar 5 cm). (c) $V-t$ curve of the all-in-one shape-adaptive self-charging power package (6 KP-SCs connected in series) under various operating modes. The circuit diagram of the all-in-one shape-adaptive self-charging power package is also shown as the inset. (d) $V-t$ curve of the all-in-one shape-adaptive self-charging power package with charging by TENG (working frequency 5 Hz). The inset shows the photograph of charging the all-in-one shape-adaptive self-charging power package by hand flapping. (e) Enlarged $V-t$ curve of the all-in-one shape-adaptive self-charging power package connected to an electric watch under various operating modes, for example, discharging mode, sustainable mode, and charging mode.

self-charging power unit for wearable/portable electronics is presented in Figure 5a. Figure 5b demonstrates an all-in-one shape-adaptive self-charging power unit under different kinds of complex deformations, including stretching, twisting, and bending. It is also worth noting that our purposed self-charging power unit is washable when it is stained, owing to all of units being perfectly sealed in the silicone rubber as the assembling material (the electric performance of the KP-SC and the SR-TENG were both measured as demonstrated in Figure S8). Hence, our proposed concept of a self-charging power unit can be a potential strategy to further build up self-charging power smart cloth. To demonstrate the practical application of an all-in-one shape-adaptive self-charging power unit, it was used for harvesting periodic flapping energy (it can be also fixed under a shoe or other part of the human body for harvesting walking or swing energy as shown in Figure S9) of a human hand and then directly powering an electronic watch. Here, since charge leakage will become significant when the KP-SC is charged under smaller current ($\sim 2 \mu\text{A}$) through the TENG to a high voltage (as shown in Figure S10a), we integrated six independent KP-SC units in series to solve this problem. Figure 5c shows the $V-t$ curve of the all-in-one shape-adaptive self-charging power package when the TENG is working under the frequency of 5 Hz and then connected with an electronic watch. The circuit diagram of the all-in-one shape-adaptive self-charging power package is also shown as the inset. At the beginning, the linear-like $V-t$ curve indicates that the all-in-one shape-adaptive self-charging power package exhibits excellent

charging performance with low charge leakage under a continuous charging process. The charging curve in the initial 20 s is enlarged, as shown in Figure 5d (the demo of the charging process is shown as the inset and in Video S3). Corresponding charging curves under various working frequencies (2–10 Hz) were also demonstrated as shown in Figure S10b. From the charging curve, we can calculate that the equivalent charging current (working frequency of 5 Hz) is $1.6 \mu\text{A}$, which is matched with the output value of Q_{SC} from previous results (Figure 4g). While the voltage of the all-in-one shape-adaptive self-charging power package is charged to ~ 1.4 V, it was used to drive the electronic watch. The enlarged $V-t$ curve under various operating modes, namely, discharging mode, sustainable mode, and recharging mode, is also shown in Figure 5e. In the discharging mode, the linear drop of $V-t$ curve indicates that the electronic watch had been powered up by the self-charging power package. The inset shows a digital photograph of the lighted electronic watch. Once we flapped the self-charging power package, the electronic watch can be sustainable powered under steady voltage (sustainable mode, ~ 5 Hz) or even charged under fast operating state (charging mode, ~ 9 Hz). A video that demonstrated the all-in-one shape-adaptive self-charging power package for powering up the electronic watch when connected with a $10 \mu\text{F}$ capacitor is shown in Video S4.

CONCLUSIONS

In summary, the concept of an all-in-one shape-adaptive self-charging power package has been demonstrated for harvesting body motion energy to sustainably drive wearable/portable electronics. By utilizing the kirigami architecture, an ultra-stretchable kirigami paper based supercapacitor with 100% stretchability and specific capacitance of ~ 1 mF/cm² and ~ 12 F/g was designed and fabricated, which shows promising electric double layer capacitance and excellent mechanical stability to be a superflexible energy storage device. By utilizing silicone rubber and Ag nanowires, an ultrastretchable and shape-adaptive TENG was fabricated with an output of ~ 160 nC per half working cycle and open-circuit voltage of ~ 250 V under stretching state of 100%. By assembling the KP-SC into the TENG with a full-wave rectifier, an all-in-one shape-adaptive SPCU was achieved for harvesting hand flapping energy and continually powering an electric watch. This work presents a prosperous advancement in the practical wearable applications of self-powered systems, which will initiate promising improvements in self-powered flexible displays and wearable electronics.

EXPERIMENTAL SECTION

Fabrication of the KP-SC for Energy Storage. In this work, sandpaper (2000 grit, 3M) was used as the substrate for fabricating the KP-SC. The rough surface morphology of sandpaper provides a high deposition area for increasing the loading amount of graphite. Meanwhile, waterproof treated sandpaper exhibits ultrafine stability for assembling the gel electrolyte. A conductive Au layer (thickness ≈ 200 nm) was deposited on the surface of the kirigami based sandpaper electrode by e-beam deposition. In this study, graphite was utilized as the active material in the KP-SC device and then directly coated on the as-prepared laser-pattern electrode by the common pencil drawing method. A Nafion (0.5% in alcohol) ionomer layer was coated on the top of the electrode to prevent graphite peeling off from the sandpaper substrate. After that, the as-prepared graphite electrode was precisely cut into kirigami architecture by laser cutter (25×50 mm²). A separator between the two graphite electrodes was also cut into same designed pattern (27×50 mm²). Finally, two as-fabricated kirigami electrodes were coated with H₃PO₄/PVA (5 g of H₃PO₄ and 5 g of PVA in 50 mL of deionized water) gel electrolyte and assembled with the kirigami separator. Hot glue was used to seal the assembly to prevent water penetration.

Fabrication of the TENG for Energy Harvesting. Ag nanowire paste (Sigma-Aldrich, diameter ≈ 115 nm and length = 20–50 μ m) was well dispersed in isopropyl alcohol solvent with the weight ratio of 0.1%. AgNW paste was uniformly coated on an acrylic sheet with a rectangle shape area (7×4 cm²) patterned by kapton tapes (25 μ m). After drying for 5 h at 30 °C, the tapes were removed from the sheet for the next fabrication process. Silicone rubber (Smooth-On, Ecoflex 00-10) was mixed with the two components in a 1:1 weight ratio. The mixed gel was cast onto the as-fabricated Ag nanowire-coated acrylic sheet at an approximate thickness of 1.5 mm. Then, the silicone rubber film with Ag nanowire layer was peeled off from the acrylic sheet after curing at 40 °C for 3 h. Finally, another 1.5 mm silicon rubber was poured and cured for assembling the Ag nanowire layer after connection with a copper tape.

Characterization and Measurement. Field emission scanning electron microscopy (Hitachi SU8010) was employed to measure the morphology of the graphite based electrode and the Ag nanowire based flexible electrode. For the electric output measurement of the TENG, a linear motor (Linmot E1100) was applied to mimic human motions, driving the TENG contact and separation. A programmable electrometer (Keithley 6514) was adopted to test the open-circuit voltage, short-circuit current, and transferred charge. The software platform is constructed based on LabView, which is capable of realizing real-time data acquisition control and analysis. The

electrochemical performance of the KP-SC was measured by an electrochemical workstation (Princeton Applied Research, VersaSTAT 3).

ASSOCIATED CONTENT

Supporting Information

The Supporting Information is available free of charge on the ACS Publications website at DOI: [10.1021/acsnano.6b06621](https://doi.org/10.1021/acsnano.6b06621).

Sandpaper based kirigami electrode, electric measurement of the basic properties of the KP-SC, electric test of KP-SC connected in series and parallel, fabrication process of silicone rubber based triboelectric nanogenerator, mechanical properties of the device, scheme of the Poisson effect, TENG for instantaneously powering several green LEDs connected in series, electric performance of the KP-SC and SR-TENG before and after washing, photographs showing the SPCU fixed under a shoe and wrapped on the arm, and charging properties of the KP-SC (PDF)

Video S1: The performance of the KP-SC while periodically stretching and releasing (AVI)

Video S2: Lighting up LED by KP-SCs connected in series while stretching (AVI)

Video S3: Charging KP-SCs by flapping TENG (AVI)

Video S4: Sustainably driving an electric watch by TENG with with a 10 μ F capacitor connected (AVI)

AUTHOR INFORMATION

Corresponding Authors

*Prof. Chenguo Hu: hucg@cqu.edu.cn.

*Prof. Zhong Lin Wang: zhong.wang@mse.gatech.edu.

ORCID

Min-Hsin Yeh: 0000-0002-6150-4750

Zhong Lin Wang: 0000-0002-5530-0380

Author Contributions

[†]H.G., M.H.Y., and Y.C.L. contributed equally to this work.

Notes

The authors declare no competing financial interest.

ACKNOWLEDGMENTS

H.G. acknowledges the fellowship from the China Scholarship Council (CSC). Research was supported by the Hightower Chair foundation, and the “thousands talents” program for pioneer researcher and his innovation team, China, National Natural Science Foundation of China (Grant Nos. 51572040, 51432005, 5151101243, and 51561145021).

REFERENCES

- (1) Chen, Y.; Au, J.; Kazlas, P.; Ritenour, A.; Gates, H.; McCreary, M. Electronic Paper: Flexible Active-Matrix Electronic Ink Display. *Nature* **2003**, *423*, 136–136.
- (2) Kim, S.; Kwon, H.-J.; Lee, S.; Shim, H.; Chun, Y.; Choi, W.; Kwack, J.; Han, D.; Song, M.; Kim, S.; Mohammadi, S.; Kee, I.; Lee, S. Y. Low-Power Flexible Organic Light-Emitting Diode Display Device. *Adv. Mater.* **2011**, *23*, 3511–3516.
- (3) Yoon, B.; Ham, D.-Y.; Yarimaga, O.; An, H.; Lee, C. W.; Kim, J.-M. Inkjet Printing of Conjugated Polymer Precursors on Paper Substrates for Colorimetric Sensing and Flexible Electrochromic Display. *Adv. Mater.* **2011**, *23*, 5492–5497.
- (4) Kim, D.-H.; Ahn, J.-H.; Choi, W. M.; Kim, H.-S.; Kim, T.-H.; Song, J.; Huang, Y. Y.; Liu, Z.; Lu, C.; Rogers, J. A. Stretchable and Foldable Silicon Integrated Circuits. *Science* **2008**, *320*, 507–511.

- (5) Hecht, D. S.; Hu, L.; Irvin, G. Emerging Transparent Electrodes Based on Thin Films of Carbon Nanotubes, Graphene, and Metallic Nanostructures. *Adv. Mater.* **2011**, *23*, 1482–1513.
- (6) Hu, L.; Kim, H. S.; Lee, J.-Y.; Peumans, P.; Cui, Y. Scalable Coating and Properties of Transparent, Flexible, Silver Nanowire Electrodes. *ACS Nano* **2010**, *4*, 2955–2963.
- (7) De, S.; Higgins, T. M.; Lyons, P. E.; Doherty, E. M.; Nirmalraj, P. N.; Blau, W. J.; Boland, J. J.; Coleman, J. N. Silver Nanowire Networks as Flexible, Transparent, Conducting Films: Extremely High DC to Optical Conductivity Ratios. *ACS Nano* **2009**, *3*, 1767–1774.
- (8) Chou, H.-H.; Nguyen, A.; Chortos, A.; To, J. W. F.; Lu, C.; Mei, J.; Kurosawa, T.; Bae, W.-G.; Tok, J. B. H.; Bao, Z. A Chameleon-Inspired Stretchable Electronic Skin with Interactive Colour Changing Controlled by Tactile Sensing. *Nat. Commun.* **2015**, *6*, 8011.
- (9) Wang, X.; Gu, Y.; Xiong, Z.; Cui, Z.; Zhang, T. Electronic Skin: Silk-Molded Flexible, Ultrasensitive, and Highly Stable Electronic Skin for Monitoring Human Physiological Signals. *Adv. Mater.* **2014**, *26*, 1309.
- (10) Hu, K.; Xiong, R.; Guo, H.; Ma, R.; Zhang, S.; Wang, Z. L.; Tsukruk, V. V. Self-Powered Electronic Skin with Biotactile Selectivity. *Adv. Mater.* **2016**, *28*, 3549–3556.
- (11) Mugele, F.; Baret, J. C. Electrowetting: from Basics to Applications. *J. Phys.: Condens. Matter* **2005**, *17*, R705–R774.
- (12) Cima, M. J. Next-Generation Wearable Electronics. *Nat. Biotechnol.* **2014**, *32*, 642–643.
- (13) Ha, M.; Park, J.; Lee, Y.; Ko, H. Triboelectric Generators and Sensors for Self-Powered Wearable Electronics. *ACS Nano* **2015**, *9*, 3421–3427.
- (14) Duan, X.; Niu, C.; Sahi, V.; Chen, J.; Parce, J. W.; Empedocles, S.; Goldman, J. L. High-Performance Thin-Film Transistors Using Semiconductor Nanowires and Nanoribbons. *Nature* **2003**, *425*, 274–278.
- (15) Yao, B.; Yuan, L.; Xiao, X.; Zhang, J.; Qi, Y.; Zhou, J.; Zhou, J.; Hu, B.; Chen, W. Paper-Based Solid-State Supercapacitors with Pencil-Drawing Graphite/Polyaniline Networks Hybrid Electrodes. *Nano Energy* **2013**, *2*, 1071–1078.
- (16) Gao, K.; Shao, Z.; Wu, X.; Wang, X.; Zhang, Y.; Wang, W.; Wang, F. Paper-based Transparent Flexible Thin Film Supercapacitors. *Nanoscale* **2013**, *5*, 5307–5311.
- (17) Wang, J. Z.; Chou, S. L.; Liu, H.; Wang, G. X.; Zhong, C.; Chew, S. Y.; Liu, H. K. Highly Flexible and Bendable Free-Standing Thin Film Polymer for Battery Application. *Mater. Lett.* **2009**, *63*, 2352–2354.
- (18) Ihlefeld, J. F.; Clem, P. G.; Doyle, B. L.; Kotula, P. G.; Fenton, K. R.; Applett, C. A. Fast Lithium-Ion Conducting Thin-Film Electrolytes Integrated Directly On Flexible Substrates for High-Power Solid-State Batteries. *Adv. Mater.* **2011**, *23*, 5663–5667.
- (19) Liu, L.; Niu, Z.; Zhang, L.; Zhou, W.; Chen, X.; Xie, S. Nanostructured Graphene Composite Papers for Highly Flexible and Foldable Supercapacitors. *Adv. Mater.* **2014**, *26*, 4855–4862.
- (20) Yu, C.; Masarapu, C.; Rong, J.; Wei, B.; Jiang, H. Stretchable Supercapacitors Based on Buckled Single-Walled Carbon-Nanotube Macrofilms. *Adv. Mater.* **2009**, *21*, 4793–4797.
- (21) Fan, F.-R.; Tian, Z.-Q.; Wang, Z. L. Flexible Triboelectric Generator. *Nano Energy* **2012**, *1*, 328–334.
- (22) Song, Z.; Ma, T.; Tang, R.; Cheng, Q.; Wang, X.; Krishnaraju, D.; Panat, R.; Chan, C. K.; Yu, H.; Jiang, H. Origami Lithium-Ion Batteries. *Nat. Commun.* **2014**, *5*, 3140.
- (23) Xu, S.; Zhang, Y.; Cho, J.; Lee, J.; Huang, X.; Jia, L.; Fan, J. A.; Su, Y.; Su, J.; Zhang, H.; Cheng, H.; Lu, B.; Yu, C.; Chuang, C.; Kim, T.; Song, T.; Shigeta, K.; Kang, S.; Dagdeviren, C.; Petrov, I.; Braun, P. V.; Huang, Y.; Paik, U.; Rogers, J. A. Stretchable Batteries with Self-Similar Serpentine Interconnects and Integrated Wireless Recharging Systems. *Nat. Commun.* **2013**, *4*, 1543.
- (24) Niu, S.; Wang, X.; Yi, F.; Zhou, Y. S.; Wang, Z. L. A Universal Self-Charging System Driven by Random Biomechanical Energy for Sustainable Operation of Mobile Electronics. *Nat. Commun.* **2015**, *6*, 8975.
- (25) Wang, X.; Song, J.; Liu, J.; Wang, Z. L. Direct Current Nanogenerator Driven by Ultrasonic Wave. *Science* **2007**, *316*, 102–105.
- (26) Qin, Y.; Wang, X.; Wang, Z. L. Microfibre-Nanowire Hybrid Structure for Energy Scavenging. *Nature* **2008**, *451*, 809–813.
- (27) Yang, R.; Qin, Y.; Dai, L.; Wang, Z. L. Power Generation with Laterally Packaged Piezoelectric Fine Wires. *Nat. Nanotechnol.* **2009**, *4*, 34–39.
- (28) Lang, S. B. Pyroelectricity: From Ancient Curiosity to Modern Imaging Tool. *Phys. Today* **2005**, *58*, 31–36.
- (29) Wen, Z.; Chen, J.; Yeh, M. H.; Guo, H.; Li, Z.; Fan, X.; Zhang, T.; Zhu, L.; Wang, Z. L. Blow-Driven Triboelectric Nanogenerator as an Active Alcohol Breath Analyzer. *Nano Energy* **2015**, *16*, 38–46.
- (30) Lee, K. Y.; Chun, J.; Lee, J. H.; Kim, K. N.; Kang, N. R.; Kim, J. Y.; Kim, M. H.; Shin, K. S.; Gupta, M. K.; Baik, J. M.; Kim, S. W. Hydrophobic Sponge Structure-Based Triboelectric Nanogenerator. *Adv. Mater.* **2014**, *26*, 5037–5042.
- (31) Zheng, Q.; Shi, B.; Fan, F.; Wang, X.; Yan, L.; Yuan, W.; Wang, S.; Liu, H.; Li, Z.; Wang, Z. L. In Vivo Powering of Pacemaker by Breathing-Driven Implanted Triboelectric Nanogenerator. *Adv. Mater.* **2014**, *26*, 5851–5856.
- (32) Guo, H.; Chen, J.; Yeh, M. H.; Fan, X.; Wen, Z.; Li, Z.; Hu, C.; Wang, Z. L. An Ultrarobust High-Performance Triboelectric Nanogenerator Based on Charge Replenishment. *ACS Nano* **2015**, *9*, 5577–5584.
- (33) Wang, J.; Li, X.; Zi, Y.; Wang, S.; Li, Z.; Zheng, L.; Yi, F.; Li, S.; Wang, Z. L. A Flexible Fiber-Based Supercapacitor-Triboelectric-Nanogenerator Power System for Wearable Electronics. *Adv. Mater.* **2015**, *27*, 4830–4836.
- (34) Wu, C.; Wang, X.; Lin, L.; Guo, H.; Wang, Z. L. Paper-Based Triboelectric Nanogenerators Made of Stretchable Interlocking Kirigami Patterns. *ACS Nano* **2016**, *10*, 4652–4659.
- (35) Yang, P. K.; Lin, L.; Yi, F.; Li, X.; Pradel, K. C.; Zi, Y.; Wu, C. I.; He, J. H.; Zhang, Y.; Wang, Z. L. A Flexible, Stretchable and Shape-Adaptive Approach for Versatile Energy Conversion and Self-Powered Biomedical Monitoring. *Adv. Mater.* **2015**, *27*, 3817–3824.
- (36) Zi, Y.; Guo, H.; Wen, Z.; Yeh, M. H.; Hu, C.; Wang, Z. L. Harvesting Low-Frequency (< 5 Hz) Irregular Mechanical Energy: A Possible Killer-Application of Triboelectric Nanogenerator. *ACS Nano* **2016**, *10*, 4797–4805.
- (37) Hou, T. C.; Yang, Y.; Zhang, H.; Chen, J.; Chen, L. J.; Wang, Z. L. Triboelectric Nanogenerator Built Inside Shoe Insole for Harvesting Walking Energy. *Nano Energy* **2013**, *2*, 856–862.
- (38) Zhou, T.; Zhang, C.; Han, C.; Fan, F.; Tang, W.; Wang, Z. L. Woven Structured Triboelectric Nanogenerator for Wearable Devices. *ACS Appl. Mater. Interfaces* **2014**, *6*, 14695–14701.
- (39) Seung, W.; Gupta, M. K.; Lee, K. Y.; Shin, K. S.; Lee, J. H.; Kim, T. Y.; Kim, S.; Lin, J.; Kim, J. H.; Kim, S. W. Nanopatterned Textile-Based Wearable Triboelectric Nanogenerator. *ACS Nano* **2015**, *9*, 3501–3509.
- (40) Guo, H.; He, X.; Zhong, J.; Zhong, Q.; Leng, Q.; Hu, C.; Chen, J.; Tian, L.; Xi, Y.; Zhou, J. A Nanogenerator for Harvesting Airflow Energy and Light Energy. *J. Mater. Chem. A* **2014**, *2*, 2079–2087.
- (41) Pu, X.; Li, L.; Song, H.; Du, C.; Zhao, Z.; Jiang, C.; Cao, G.; Hu, W.; Wang, Z. L. A Self-Charging Power Unit by Integration of a Textile Triboelectric Nanogenerator and a Flexible Lithium-Ion Battery for Wearable Electronics. *Adv. Mater.* **2015**, *27*, 2472–2478.
- (42) Wang, S.; Lin, Z. H.; Niu, S.; Lin, L.; Xie, Y.; Pradel, K. C.; Wang, Z. L. Motion Charged Battery as Sustainable Flexible-Power-Unit. *ACS Nano* **2013**, *7*, 11263–11271.
- (43) Bles, M. K.; Barnard, A. W.; Rose, P. A.; Roberts, S. P.; McGill, K. L.; Huang, P. Y.; Ruyack, A. R.; Kevek, J. W.; Kobrin, B.; Muller, D. A.; McEuen, P. L. Graphene Kirigami. *Nature* **2015**, *524*, 204–207.
- (44) Shyu, T. C.; Damasceno, P. F.; Dodd, P. M.; Lamoureux, A.; Xu, L.; Shlian, M.; Shtein, M.; Glotzer, S. C.; Kotov, N. A. A Kirigami Approach to Engineering Elasticity in Nanocomposites Through Patterned Defects. *Nat. Mater.* **2015**, *14*, 785–789.

- (45) Lamoureux, A.; Lee, K.; Shlian, M.; Forrest, S. R.; Shtein, M. Dynamic Kirigami Structures for Integrated Solar Tracking. *Nat. Commun.* **2015**, *6*, 8092.
- (46) Zheng, G.; Hu, L.; Wu, H.; Xie, X.; Cui, Y. Paper Supercapacitors by a Solvent-Free Drawing Method. *Energy Environ. Sci.* **2011**, *4*, 3368–3373.
- (47) Cheng, X.; Meng, B.; Zhang, X.; Han, M.; Su, Z.; Zhang, H. Wearable Electrode-Free Triboelectric Generator for Harvesting Biomechanical Energy. *Nano Energy* **2015**, *12*, 19–25.
- (48) Chen, J.; Guo, H.; He, X.; Liu, G.; Xi, Y.; Shi, H.; Hu, C. Enhancing Performance of Triboelectric Nanogenerator by Filling High Dielectric Nanoparticles into Sponge PDMS Film. *ACS Appl. Mater. Interfaces* **2016**, *8*, 736–744.
- (49) Zi, Y.; Niu, S.; Wang, J.; Wen, Z.; Tang, W.; Wang, Z. L. Standards and Figure-Of-Merits for Quantifying the Performance of Triboelectric Nanogenerators. *Nat. Commun.* **2015**, *6*, 8376.